Scientific Reports

https://doi.org/10.1038/s41598-026-61524-4

Article in Press

Single pass inactivation of airborne multidrug resistant bacteria using electron beam irradiation with mechanistic evidence

Received: 26 March 2026

Accepted: 6 July 2026

Published online: 21 July 2026

Cite this article as: Seza A., Mozahheb Yousefi K., Saeedifar S. *et al.* Single pass inactivation of airborne multidrug resistant bacteria using electron beam irradiation with mechanistic evidence. *Sci Rep* (2026). https://doi.org/10.1038/s41598-026-61524-4

Ashkan Seza, Kimia Mozahheb Yousefi, Sara Saeedifar & Sara Minaeian

We are providing an unedited version of this manuscript to give early access to its findings. Before final publication, the manuscript will undergo further editing. Please note there may be errors present which affect the content, and all legal disclaimers apply.

If this paper is publishing under a Transparent Peer Review model then Peer Review reports will publish with the final article.

ARTICLE IN PRESS

© The Author(s) 2026. **Open Access** This article is licensed under a Creative Commons Attribution-NonCommercial-NoDerivatives 4.0 International License, which permits any non-commercial use, sharing, distribution and reproduction in any medium or format, as long as you give appropriate credit to the original author(s) and the source, provide a link to the Creative Commons licence, and indicate if you modified the licensed material. You do not have permission under this licence to share adapted material derived from this article or parts of it. The images or other third party material in this article are included in the article's Creative Commons licence, unless indicated otherwise in a credit line to the material. If material is not included in the article's Creative Commons licence and your intended use is not permitted by statutory regulation or exceeds the permitted use, you will need to obtain permission directly from the copyright holder. To view a copy of this licence, visit http://creativecommons.org/licenses/by-nc-nd/4.0/.

ARTICLE IN PRESS

Single Pass Inactivation of Airborne Multidrug Resistant Bacteria Using Electron Beam Irradiation with Mechanistic Evidence

Authors:

Ashkan Seza[1], Kimia Mozahheb Yousefi[1,2], Sara Saeedifar[1], Sara Minaeian[1*]

1. Antimicrobial Resistance Research Center, Institute of Immunology and Infectious Diseases, Iran University of Medical Sciences, Tehran, Iran.
2. Faculty of Medicine, Iran University of Medical Sciences, Tehran, Iran.

***Corresponding author:** Sara Minaeian (sara.minaeian@gmail.com)

ARTICLE IN PRESS

Abstract

Airborne and aerosol transmission of multidrug-resistant (MDR) bacteria pose a major challenge in healthcare environments. This study evaluated the performance of an electron-beam irradiation (EBI) system for inactivating airborne MDR bacteria under controlled laboratory conditions. To perform this assessment, clinical isolates of MDR *Pseudomonas aeruginosa*, *Acinetobacter* sp., *Klebsiella* sp., and methicillin-resistant *Staphylococcus aureus* (MRSA) were aerosolized to simulate realistic airborne transmission and subsequently introduced into the EBI system. Downstream bacterial aerosols were collected using liquid impingers and quantified by culture-based enumeration. CFU data were $\log_{10}$-transformed prior to analysis. The EBI system reduced airborne bacterial loads by 4.01

ARTICLE IN PRESS

log_{10} for *P. aeruginosa*, 3.64 log_{10} for *Acinetobacter* sp., 3.64 log_{10} for *Klebsiella* sp., and 5.37 log_{10} for MRSA, corresponding to disinfection efficiencies of 99.98–99.999%. Scanning electron microscopy (SEM) and elemental mechanistic study revealed morphological damage, including membrane rupture, surface collapse, and loss of structural integrity, suggesting that electron impact and electroporation may be major mechanisms of inactivation.

These results demonstrate that EBI is a rapid and effective method for mitigating airborne MDR bacterial threats, with potential for deployment in healthcare, laboratory, and other high-risk indoor environments.

Keywords:

Electron-beam irradiation, EBI, Airborne transmission, Aerosolized bacteria, Electron-induced membrane disruption, Electroporation, Multidrug-resistant bacteria, MDR, Bioaerosol inactivation, Bacteria elemental analysis, Scanning electron microscopy, SEM

ARTICLE IN PRESS

1. Introduction

Healthcare-associated infections (HAIs) remain a critical public health issue, representing one of the most significant contributors to morbidity and mortality in modern healthcare [1]. Airborne transmission of multidrug-resistant (MDR) bacteria amplifies this challenge by undermining traditional infection control measures within healthcare environments [2,3]. These pathogens account for a significant proportion of nosocomial infections,

ARTICLE IN PRESS

leading to prolonged hospital stays, elevated treatment costs, and increased mortality rates, particularly among immune-compromised patients [4–6]. Common MDR pathogens such as *Pseudomonas aeruginosa*, *Acinetobacter* species, *Klebsiella* species, and methicillin-resistant *Staphylococcus aureus* (MRSA) can persist in hospital air and on environmental surfaces, spreading via aerosolization and contact with inadequately disinfected areas [7–9]. In enclosed healthcare settings with poor ventilation, these microorganisms can form stable airborne reservoirs, substantially heightening the risk of hospital-acquired infections and localized outbreaks [10,11]. Conventional air purification technologies, such as High-Efficiency Particulate Air (HEPA) filtration, capture airborne particles as small as 0.3 μm with 99.97% efficiency; however, their effectiveness is limited to mechanical trapping rather than microbial inactivation [12,13]. Pathogens retained on filter surfaces can remain viable, creating a potential source for re-aerosolization or cross-contamination during filter maintenance and replacement [14,15]. Moreover, HEPA systems require high installation and operational costs, frequent maintenance, and exhibit reduced performance in humid environments [16,17]. They also show limited efficiency against smaller virus-containing particles and lack real-time pathogen neutralization capability [18,19]. These drawbacks underscore the need for innovative air disinfection technologies capable of both capturing and actively inactivating microorganisms *in situ* [20,21]. To address these limitations, several advanced air purification strategies have been explored, including

ARTICLE IN PRESS

ultraviolet germicidal irradiation (UVGI), electrostatic precipitation, photocatalytic oxidation, and non-thermal plasma systems [22–25]. Among these emerging technologies, electrically driven systems such as non-thermal plasma and electron-based disinfection methods offer distinct advantages by producing physical and electrical effects capable of directly disrupting microbial structures [26,27].

The EBI system evaluated in this study generates high-energy electrons that can directly damage microbial cell envelopes through electron impact and can also induce electroporation via intense localized electric fields, leading to irreversible membrane destabilization and cell death [28]. The single-pass air disinfection efficacy of the EBI system was tested using a controlled aerosolization laboratory model, to quantify the single-pass inactivation efficiency and $\log_{10}$ reductions of aerosolized MDR bacteria of multidrug-resistant (MDR) bacteria, including *P. aeruginosa, Acinetobacter* species*, Klebsiella* species, and methicillin-resistant *S. aureus* (MRSA), isolated from clinical samples obtained at Hazrat Rasoul Hospital, Tehran, Iran. The findings from this study will inform the future application and use of electron-beam irradiation as an air-disinfection technology for enhancing indoor microbial air quality and strengthening infection-control strategies in healthcare and other critical indoor environments, addressing the urgent need for alternative and novel disinfection approaches to address the escalating threat of antimicrobial resistance.

2. Materials and methods

ARTICLE IN PRESS

2.1 Bacterial isolates and Antibiogram Profiles

Clinical isolates of *Acinetobacter* sp*., S. aureus*, *Klebsiella* and *P. aeruginosa* were obtained from Hazrat-e Rasoul Hospital in Tehran, Iran. These isolates were selected based on their demonstrated resistance to multiple antibiotic classes (Table 1). Antibiogram testing was performed using the Kirby-Bauer disk diffusion method in accordance with CLSI M100 guidelines (2023). All experiments and methods were performed in accordance with relevant guidelines and regulations. The study protocols and the use of clinical isolates were reviewed and approved by the Ethics Committee of Iran University of Medical Sciences (Approval ID: IR.IUMS.REC.1403.958). Informed consent was obtained from all subjects and/or their legal guardian(s). All isolates were completely anonymized to protect patient privacy.

ARTICLE IN PRESS

Table 1: Antibiogram profiles of multidrug-resistant (MDR) clinical isolates used in the study.

Microorganism	Sensitive (S)	Resistant (R)
***Acinetobacter* sp.**	—	Ampicillin – Sulbactam (10/10 µg), Ciprofloxacin (5 µg), Cefepime (30 µg), Ceftriaxone (30 µg), Amikacin (30 µg), Gentamicin (10 µg) , Trimethoprim –

ARTICLE IN PRESS

		Sulfamethoxazole (1.25/23.75µg), Piperacillin – Tazobactam (100/10 µg), Doxycycline (30 µg),
***Staphylococcus aureus* (MRSA)**	Linezolid (30 µg), Doxycycline (30 µg), Trimethoprim – Sulfamethoxazole (1.25/23.75µg)	Ciprofloxacin (5 µg), Clindamycin (2 µg), Erythromycin (15 µg), Cefoxitin (30µg), Penicillin G (10 U), Vancomycin (30 µg),
***Klebsiella* sp.**	—	Doxycycline (30 µg), Gentamicin (10 µg), Amikacin (30 µg), Ciprofloxacin (5 µg), Imipenem (10 µg), Meropenem (10 µg), ,Piperacillin – Tazobactam(100/10 µg), Ampicillin–Sulbactam (10/10 µg),
Pseudomonas aeruginosa	Gentamicin (10 µg), Amikacin (30 µg)	Piperacillin – Tazobactam (100/10 µg), Cefazolin (30 µg), Cefepime (30 µg), Ciprofloxacin (5 µg), Imipenem (10 µg), Meropenem (10 µg),

ARTICLE IN PRESS

ARTICLE IN PRESS

2.2 Bacterial Culture Preparation and Inoculum Standardization

Acinetobacter sp*., S. aureus, Klebsiella* sp., and *P. aeruginosa* cultures were grown on nutrient agar at 37 °C for 24 h, then transferred to Mueller–Hinton (MH) broth and incubated in a shaker incubator at 37 °C for 2 h to obtain a viable, standardized inoculum. Bacterial concentrations were adjusted to approximately 10^9CFU/mL based on optical density at 600 nm (OD_{600}) using a spectrophotometer. The cultures were then centrifuged and resuspended in 0.9% physiological saline (Merck, Germany). Cell density was further standardized using McFarland standards, and serial dilutions were prepared. To confirm the final cell concentration, serial dilutions were spread-plated on nutrient agar and colony-forming units (CFU) were enumerated.

ARTICLE IN PRESS

2.3 Experimental Setup

The device used in this study is an air-cleaning system with multiple layers of electron beam emitters within a stainless-steel reactor (Model MD250, PlasmaShield Ltd, Australia). The device was incorporated into the experimental setup shown in Figure 1. Microorganisms were aerosolized using a 3-jet Collison nebulizer (CH Technologies, Westwood, NJ, USA) at an inoculum suspension concentration of 10^9 CFU/mL in 0.9% (w/v) physiological saline (Merck, Germany). The nebulizer was positioned at the start of a detachable stainless-steel pipeline (25 cm diameter, 70 cm length) before entering the device. Airflow within the duct was maintained at 1 m/s,

ARTICLE IN PRESS

and nebulization was achieved using compressed air at a flow rate of 14 L/min. Aerosol generation was performed continuously for 30 minutes.

Microorganisms downstream of the EBI unit were collected 120 cm beyond the reactor outlet using three glass impingers (Unilab, 500 mL, borosilicate glass 3.3) positioned inside the stainless-steel pipe at 120° intervals. Each impinger operated at 26.67 L/min simultaneously with the nebulizer for 30 minutes using 0.9% saline as the collection medium. The impinger located at the center of the pipe consistently showed the highest collection efficiency and was therefore selected for serial dilutions and CFU enumeration in all experiments. The other two impingers were used to verify aerosol uniformity across the duct cross-section.

Aerosol uniformity was confirmed through preliminary experiments, where CFU counts from the three impingers showed good agreement (typically within ± 0.3–0.5 $\log_{10}$ variation across replicates). In the final triplicate experiments, the coefficient of variation (CV) among the three impingers in control runs was less than 25% for all tested microorganisms, confirming acceptable uniformity of aerosol distribution. Only data from the central (highest-yield) impinger were used for quantitative analysis to ensure maximum recovery and consistency. Prior to the main triplicate experiments, multiple preliminary runs were conducted under identical conditions to optimize and verify the stability of the aerosol generation and sampling setup. The system was allowed to equilibrate for several minutes after starting nebulization before formal sampling began. All experiments

ARTICLE IN PRESS

were performed under controlled laboratory conditions with an average temperature of 28 ± 0.8 °C measured continuously at the chamber inlet. Collected samples were serially diluted in physiological saline, and 100 µL of each dilution was spread-plated onto nutrient agar plates in triplicate, and incubated at 37 °C for 24 h prior to CFU enumeration. Each testing condition was conducted in triplicate. Conditions included the EBI turned on and also a negative control where the device was replaced with an empty casing. This was repeated for each microorganism concentration.

The experimental setup consisted of a closed-loop stainless-steel duct system. All connections between the nebulizer, stainless-steel piping, EBI reactor (or empty casing for control), and downstream sampling section were sealed with silicone gaskets and clamps to minimize aerosol leakage. The system operated under slight negative pressure generated by the vacuum pumps connected to the impingers, with the majority of the airflow being drawn through the three impingers. Any excess air was exhausted through a HEPA-filtered outlet to prevent environmental contamination.

To account for potential physical losses (e.g., wall deposition or transport inefficiencies), negative control experiments (EBI device replaced with an empty casing of identical dimensions) were performed under identical conditions for each microorganism. The $\log_{10}$ reductions reported in this study represent the difference between the empty-casing control and the active EBI condition, thereby isolating the inactivation effect of the electron-beam irradiation from non-biological aerosol losses.

ARTICLE IN PRESS

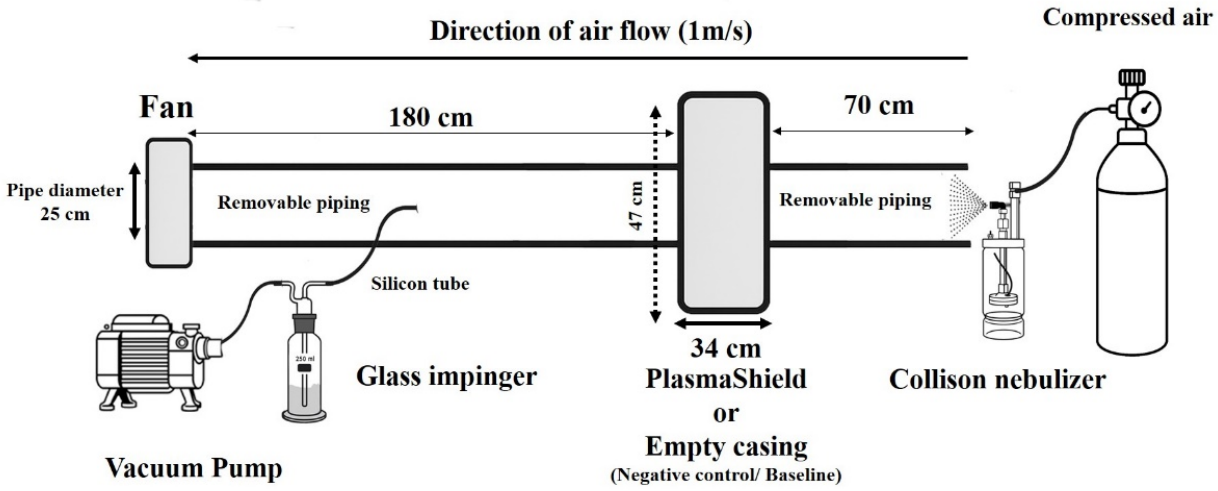


Figure 1. Schematic of experimental setup.

2.4. Statistical analysis

Statistical analysis was performed using IBM SPSS Statistics (version 27). Because microbial count data typically follow a log-normal distribution, raw CFU counts were $\log_{10}$-transformed prior to calculation of means and standard deviations to achieve normality and homogeneity of variance. All results are therefore reported as mean $\log_{10}$ (CFU) ± SD.

For each microorganism, differences between control (device off) and EBI-treated (device on) groups were compared using independent samples t-tests. Statistical significance was set at $p < 0.05$. Log_{10} reductions were calculated as the arithmetic difference between the mean $\log_{10}$ (CFU) values of the control and EBI-treated samples. Disinfection efficacy (%) was calculated from the back-transformed CFU values corresponding to the

ARTICLE IN PRESS

reported $\log_{10}$ means. Samples with no detectable colony growth were assigned a value of 1 CFU prior to $\log_{10}$ transformation.

.2.5. Scanning Electron Microscopy (SEM)

SEM analysis was performed to visualize the morphological alterations of multi-drug resistant (MDR) bacteria following exposure to electron beam irradiation. The experiments for both control and EBI-treated samples were conducted using the full experimental setup (nebulization, duct transport, and impinger collection). For controls, the EBI device was replaced with an empty casing while all other conditions remained identical.

Microorganisms captured in the liquid impinger were carefully deposited onto pre-cleaned glass slides and immediately fixed in a 2.5% glutaraldehyde solution prepared in physiological saline at 25 °C for 24 hours to preserve cellular structures. After fixation, the glutaraldehyde solution was discarded, and the samples were sequentially dehydrated in graded ethanol solutions (70%, 90%, and 100%), each for 15 minutes, to ensure complete removal of water. The dehydrated slides were subsequently mounted on aluminum SEM stubs using conductive carbon adhesive tape and sputter-coated with a 5 nm gold layer using an NSC DSR1 sputter coater to enhance surface conductivity and imaging quality. Imaging was performed using a Mira 3 (Tescan, Czech Republic) scanning electron microscope operated at an accelerating voltage of 15 kV under high vacuum conditions. Elemental characterization of the same samples was carried out by energy dispersive X-ray spectroscopy (EDS) using Aztec

ARTICLE IN PRESS

software (Oxford Instruments, UK) to evaluate surface elemental composition and detect chemical alterations associated with bacterial planktonic structures after EBI treatment.

3. Results

The single-pass disinfection performance of the EBI system against aerosolized multidrug-resistant (MDR) bacteria is summarized in Table 2 and visualized in Figure 2. The EBI system achieved mean $\log_{10}$ reductions of 4.01 for *P. aeruginosa*, 3.64 for *Acinetobacter* sp., 3.64 for *Klebsiella* sp., and 5.37 for *S. aureus* (MRSA), corresponding to disinfection efficiencies of 99.98–99.999%. The highest inactivation was observed for MRSA.

Table 2: Quantitative single-pass disinfection performance of the electron-beam irradiation (EBI) system against aerosolized multidrug-resistant (MDR) bacteria. Results are reported as mean $\log_{10}$ (CFU) ± SD for control (device off) and EBI-treated (device on) conditions obtained from triplicate experiments ($n = 3$ per condition). Log_{10} reductions were calculated as the difference between mean control and treated $\log_{10}$ (CFU) values. Disinfection efficacy (%) was calculated from CFU values derived from $\log_{10}$-transformed data. Samples with no detectable colony growth were assigned a value of 1 CFU prior to $\log_{10}$ transformation.

MDR pathogen tested	Control $\log_{10}$(CFU) ± SD	EBI $\log_{10}$(CFU) ± SD	P value	Disinfection efficacy (%)	Mean Log_{10} reduction
Pseudomonas aeruginosa	4.65 ± 0.43	0.64 ± 1.11	<0.001	99.99	4.01
Acinetobacter	5.64 ± 0.08	2.01 ± 1.75	0.06	99.98	3.64

ARTICLE IN PRESS

Klebsiella	5.39 ± 0.14	1.75 ± 1.55	0.054	99.98	3.64
Staphylococcus aureus (MRSA)	6.22 ± 0.28	0.84 ± 1.46	0.02	99.999	5.37

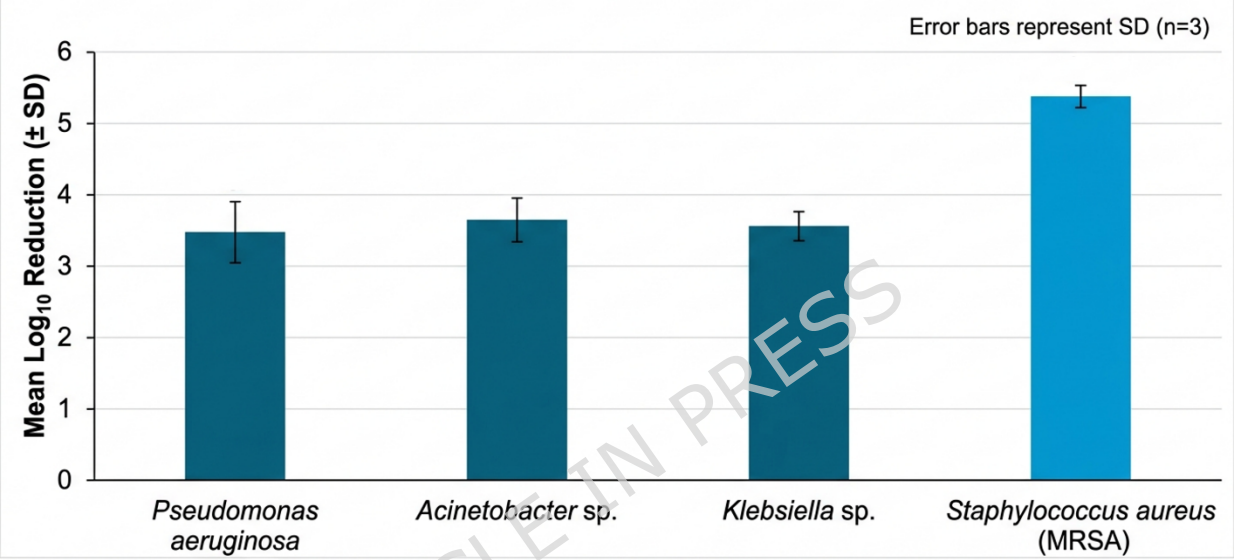


Figure 2. Single-pass $\log_{10}$ reduction of aerosolized multidrug-resistant bacteria achieved by the EBI system. Bars represent the mean ± SD (n = 3). MRSA exhibited the highest inactivation efficiency compared to the other tested species. Detailed p-values for control versus EBI comparisons are presented in Table 2.

To complement these quantitative findings, scanning electron microscopy (SEM) and energy-dispersive X-ray spectroscopy (EDS) were performed to examine electron beam induced morphological and compositional alterations in representative bacterial species, as described in the following sections.

ARTICLE IN PRESS

Figure 3 presents scanning electron micrographs (SEM) of untreated (control) and EBI-treated multidrug-resistant (MDR) bacterial species, including *P. aeruginosa* (A–B), *S. aureus* (MRSA). (C–D), *Klebsiella* sp. (E–F), and *Acinetobacter* sp. (G–H). The control panels (A, C, E, G) show the characteristic morphology of viable cells after undergoing the complete aerosolization and impinger collection process (device off).*P. aeruginosa* and *Klebsiella* sp. display smooth rod-shaped structures with intact outer membranes; *S. aureus* appears as spherical cocci with well-defined, continuous surfaces; and *Acinetobacter* sp. exhibits compact, oval-shaped cells with uniform texture, features typical of healthy, actively growing bacteria. In contrast, the EBI-treated panels (B, D, F, H) reveal extensive structural collapse and severe morphological distortion across all species. The treated *P. aeruginosa* and *Klebsiella* sp. cells exhibit extensive surface rupture and elongation collapse, indicating envelope disintegration and cytoplasmic leakage. *S. aureus* cells lose their spherical integrity and transform into fragmented, porous remnants, while *Acinetobacter* sp. appears as completely disintegrated aggregates with loss of cellular definition. These profound deformations confirm that electron beam exposure leads to irreversible physical damage of bacterial envelopes [29–31].

ARTICLE IN PRESS

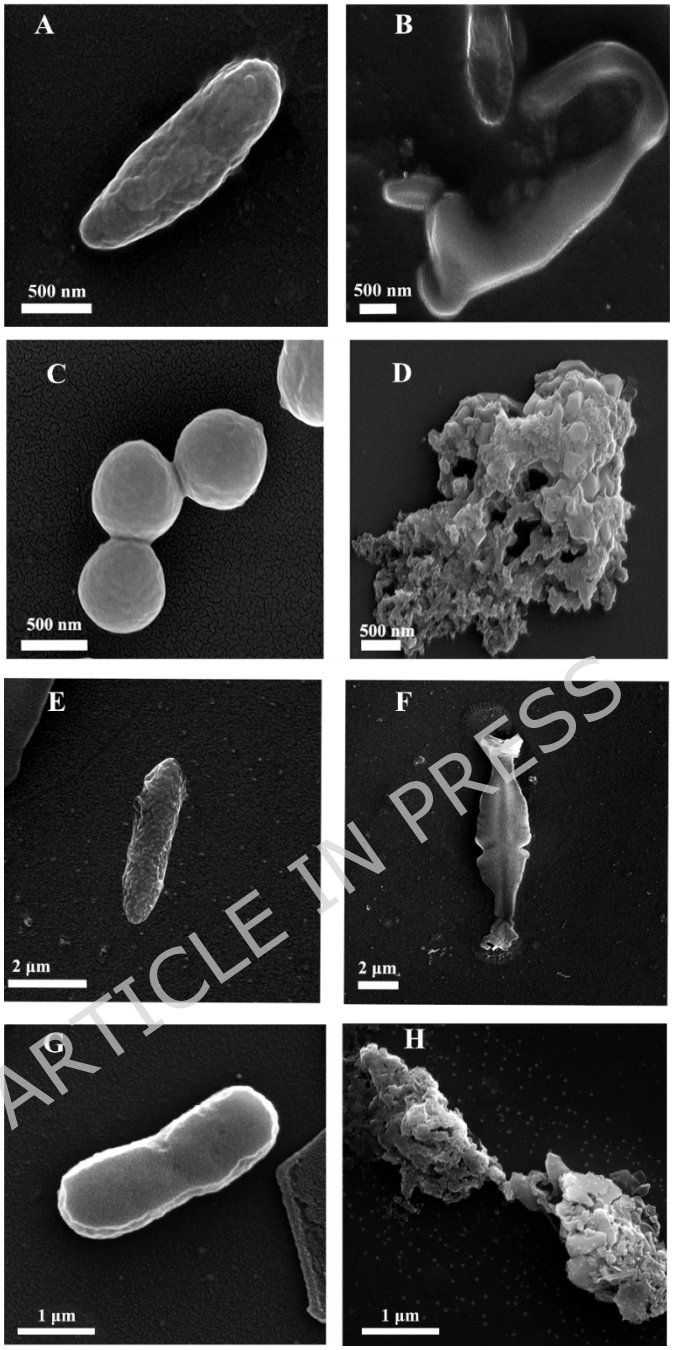
The observed destruction pattern is consistent with electron induced damage, a primary mechanism in the EBI's technology. The electrons generated by the electron-beam emitters collide directly with microbial cell

ARTICLE IN PRESS

walls, causing localized bond scission, surface sputtering, and nano-scale ablation of membrane biomolecules. This exposure disrupts lipid bilayers, peptidoglycan structures, and protein matrices, resulting in envelope perforation, membrane collapse, and eventual cellular implosion. The electron impact is further intensified by transient electroporation which accelerates structural breakdown. Together, the SEM evidence in Figure 2 demonstrates that the EBI system exerts a direct electron-mediated physical destruction effect on both Gram-positive and Gram-negative MDR bacteria. This supports the quantitative results presented in Table 2 and confirms that the predominant inactivation mechanism is physical ablation through electron impact rather than other mechanisms [32–35].

ARTICLE IN PRESS

ARTICLE IN PRESS



ARTICLE IN PRESS

Figure 3. Scanning electron microscope images of baseline/negative control (A) Pseudomonas aeruginosa (C) Staphylococcus aureus (E) Klebsiella sp and (G) Acinetobacter sp. and EBI destroyed microorganisms (B) P. aeruginosa (D) S. aureus (F) Klebsiella sp. and (H) Acinetobacter sp.

Following the extensive evidence of electron impact–driven physical ablation presented in Figure 3, further analysis was conducted to explore

ARTICLE IN PRESS

additional EBI-induced damage pathways contributing to microbial inactivation. While collision with high-speed electrons primarily causes surface erosion and molecular ablation, the intense electric fields generated within the EBI's discharge zone are also capable of inducing electroporation, a complementary mechanism that destabilizes bacterial membranes at the nanostructural level [36]. To visualize this process, the morphological effects of electron beam exposure on *P. aeruginosa* and *S. aureus* (MRSA) were examined by SEM, as shown in Figure 4.

Figure 4 presents scanning electron micrographs (SEMs) depicting the morphological alterations of *P. aeruginosa* (A–B) and *S. aureus* (MRSA) (C–D) following exposure to high-speed electrons. The control panels (A, C) show typical intact morphology: *P. aeruginosa* cells exhibit smooth, rod-shaped surfaces with clearly defined envelopes, while MRSA appears as regular spherical cocci with continuous cell walls and well-preserved contours. In contrast, the treated cells (B, D) display distinct electroporation-induced structural damage. *P. aeruginosa* demonstrates localized membrane perforations, shallow depressions, and early signs of cell wall rupture, suggesting the formation of pores caused by the intense electric field generated within the electron discharge zone. Similarly, MRSA cells reveal partial collapse and the appearance of nanoscale pits and ruptures on the surface morphological evidence of electrical membrane destabilization and pore coalescence [37–39].

ARTICLE IN PRESS

ARTICLE IN PRESS

These deformations are characteristic of irreversible electroporation, a key antimicrobial mechanism of the EBI system. The device generates an intense electric field that induces transmembrane potential differences exceeding the dielectric threshold of bacterial membranes (typically > 1 V), resulting in the formation of transient nanopores. Under sustained exposure, these pores expand irreversibly, causing leakage of intracellular components, disruption of osmotic balance, and eventual cell death. The electroporation effect is further amplified by simultaneous high-energy electron collisions within the device reactor, which together accelerate the breakdown of the phospholipid bilayer and peptidoglycan structures [31,34,40,41].

Collectively, the SEM findings in Figure 4 confirm that electroporation-driven membrane perforation is a primary mechanism of inactivation in both Gram-negative (*Pseudomonas*) and Gram-positive (*S. aureus*) bacteria. This supports the earlier electron-impact mechanism and highlights the dual-action behavior of the EBI technology, where electrical and physical destructive processes work together to produce rapid, irreversible microbial inactivation.

ARTICLE IN PRESS

ARTICLE IN PRESS

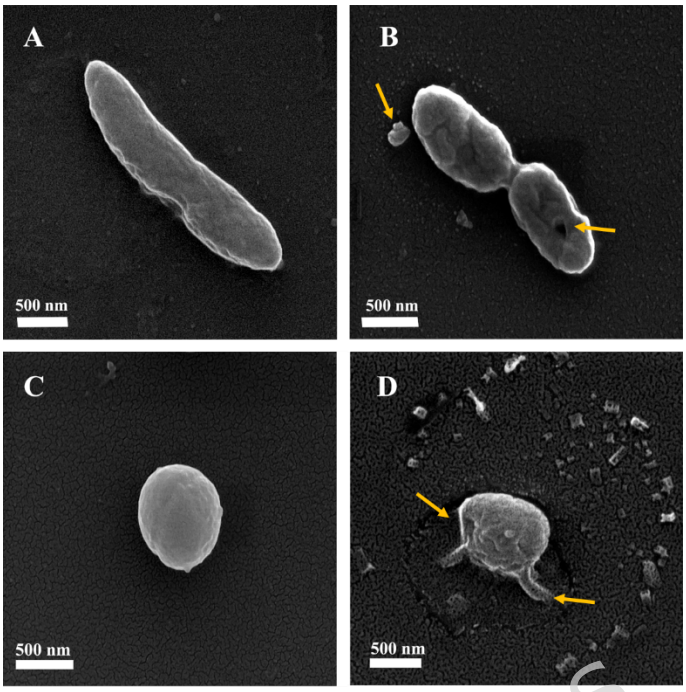


Figure 4. SEM images of P. aeruginosa (A–B) and S aureus (MRSA) (C–D) before and after EBI exposure. Electron beam-treated cells show nano-scale perforations and deformation caused by electroporation and membrane destabilization.

To further support the morphological observations and demonstrate that the observed damage is widespread, scanning electron microscopy (SEM) and energy-dispersive X-ray spectroscopy (EDS) were conducted on multidrug-resistant (MDR) Acinetobacter sp. cells exposed to EBI (Figure 5). Low-magnification images confirmed that severe structural damage was not limited to individual cells but occurred across bacterial populations.

In Figure 5A, the untreated control cells exhibit a smooth, intact morphology with an elemental composition of 60.57 wt% C, 13.39 wt% O, 9.52 wt% Si, 0.59 wt% Mg, and 0.41 wt% Al, indicative of a carbon-rich, protein–lipid envelope with negligible substrate exposure [42].

ARTICLE IN PRESS

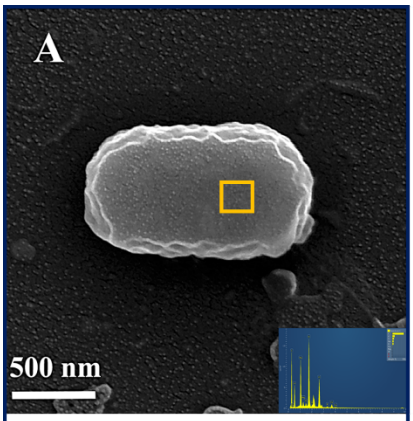
After electron beam exposure, Figure 5B shows localized membrane deformation and the formation of a central crater. Corresponding EDS spectra display 53.27 wt% C (−7.30 wt%), 22.60 wt% O (+9.21 wt%), 11.62 wt% Si (+2.10 wt%), 0.81 wt% Mg, and 0.46 wt% Al, suggesting partial oxidation, focal organic loss, and incipient exposure of the underlying glass slide substrate.

In contrast, Figure 5C reveals severe surface erosion and fragmentation. EDS analysis shows 23.06 wt% C (−37.51 wt% vs. control), 34.49 wt% O (+21.10 wt%), 21.81 wt% Si (+12.29 wt%), 1.58 wt% Mg, and 0.78 wt% Al, signifying extensive ablation of organic components and greater exposure of the inorganic glass substrate. Low-magnification images (Figure 5D–E) further confirmed that the damage was widespread. EDS spectra acquired from these fields also showed consistent trends of substantial carbon depletion and increases in oxygen and silicon signals.

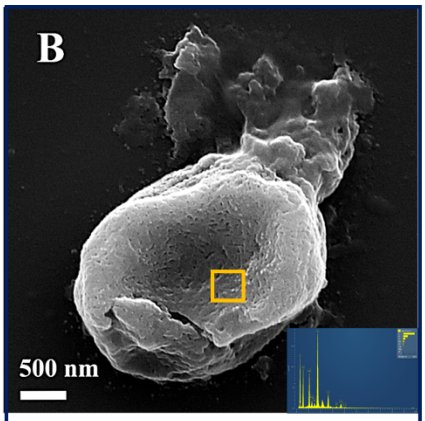
ARTICLE IN PRESS

As bacterial cells were deposited directly onto glass slides (with no mediating layer such as carbon tape between the bacteria and the glass substrate), progressive destruction of the cells resulted in increased exposure of the silicon-rich glass substrate to the electron beam. These features are consistent with a dual-mechanism pathway involving electroporation-driven membrane disruption and electron impact-induced ablation [38, 43–46]. However, due to potential substrate contributions and sample heterogeneity, the EDS data are interpreted as qualitative supportive trends rather than definitive quantitative measurements.

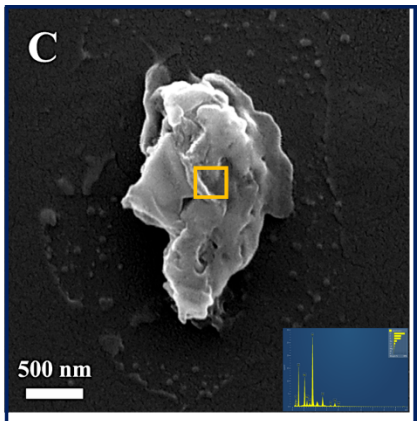
ARTICLE IN PRESS



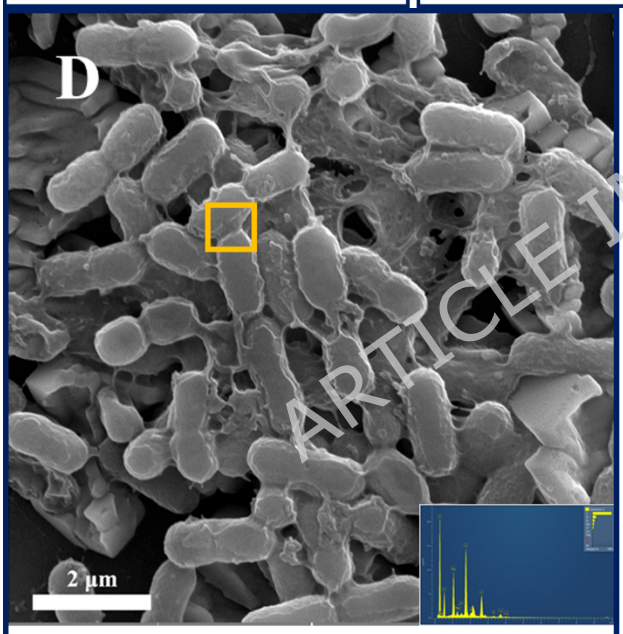
Element	Wt%
C	60.57
O	13.39
Si	9.52
Mg	0.59
Al	0.41



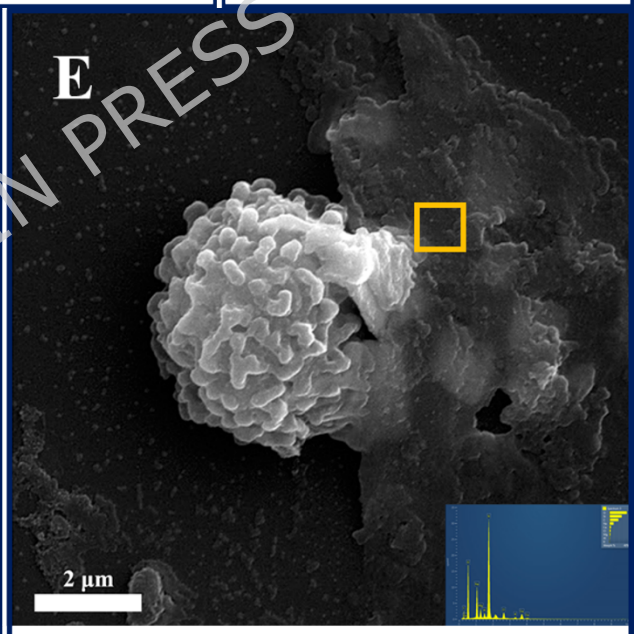
Element	Wt%
C	53.27
O	22.60
Si	11.62
Mg	0.81
Al	0.46



Element	Wt%
C	23.06
O	34.49
Si	21.81
Mg	1.58
Al	0.78



Element	Wt%
C	67.51
O	12.89
Si	7.81
Mg	0.47
Al	0.26



Element	Wt%
C	18.79
O	36.76
Si	25.85
Mg	2.16
Al	1.05

ARTICLE IN PRESS

ARTICLE IN PRESS

Figure 5. Scanning electron micrographs and EDS analysis of MDR Acinetobacter sp. (A–C) High-magnification images showing progressive cellular damage after EBI exposure. (A) Untreated control showing typical intact rod-shaped morphology. (B) Moderate damage with crater formation. (C) Severe surface erosion and fragmentation. (D–E) Low-magnification images demonstrating that the damage is widespread across the bacterial population. (D) Untreated control. (E) EBI-treated sample showing extensive structural destruction. Yellow boxes indicate representative areas selected for EDS analysis. EDS spectra acquired from multiple regions showed consistent trends of carbon depletion and increased silicon and oxygen signals in treated samples.

Although this study primarily relied on culture-based enumeration to quantify viable bacteria, all $\log_{10}$ reductions were calculated relative to matched negative controls (empty casing) conducted under identical conditions of nebulization, duct transport, and impinger collection. This approach effectively accounts for potential physical aerosol losses and transport inefficiencies. Furthermore, extensive SEM imaging, including low-magnification views (Figures 3 and 5), provides compelling visual evidence of widespread physical destruction of bacterial cells, including membrane rupture, cytoplasmic leakage, and structural collapse. These morphological observations strongly support that the observed reductions in CFU counts reflect genuine microbial inactivation rather than incomplete aerosol recovery.

ARTICLE IN PRESS

4. Discussion

The EBI air-cleaning system demonstrated high efficacy in inactivating aerosolized multidrug-resistant (MDR) bacteria, including *Staphylococcus aureus* (MRSA), *Pseudomonas aeruginosa*, *Klebsiella* sp., and *Acinetobacter* sp., under controlled laboratory conditions. The system achieved robust single-pass disinfection performance, with mean $\log_{10}$ reductions ranging from 3.64 to 5.37, corresponding to disinfection efficiencies of 99.98–

ARTICLE IN PRESS

99.999% (summarized in Table 2 and visualized in Figure 2). The highest inactivation was observed for MRSA and P. aeruginosa, with mean $\log_{10}$ reductions of 5.37 and 4.01, respectively, while *Klebsiella* sp. and *Acinetobacter* sp. exhibited mean $\log_{10}$ reductions of 3.64.

Independent samples t-tests showed statistically significant reductions for P. aeruginosa ($p < 0.001$) and MRSA ($p = 0.02$). The reductions observed for Acinetobacter sp. ($p = 0.06$) and Klebsiella sp. ($p = 0.054$) approached but did not reach the conventional significance threshold. Nevertheless, when combined with the consistent morphological damage observed by SEM across all species, these results support a broad susceptibility of MDR bacteria to EBI. SEM and EDS analyses revealed morphological and compositional changes consistent with significant cellular damage following EBI exposure. These observations support the hypothesis that electron impact and electroporation may contribute to bacterial inactivation. Specifically, the images showed severe structural deformation, membrane rupture, and loss of cellular integrity, while EDS indicated trends of carbon depletion and oxygen enrichment.

These findings are further illustrated by the schematic in Figure 6, which presents a proposed dual-action antimicrobial mechanism of the EBI system: high-energy electron impact may cause ablation of the bacterial envelope, whereas intense electric fields may induce electroporation, creating nanoscale membrane pores. In combination, these processes

ARTICLE IN PRESS

appear to accelerate cytoplasmic leakage, structural collapse, and eventual cell death. When considered alongside the quantitative reductions observed in aerosolized MDR bacteria, the morphological and elemental findings are more consistent with EBI-driven inactivation arising primarily from physical and electrical disruption than from chemical oxidation. However, the present data do not allow firm conclusions regarding the exact contribution of each mechanism, and further studies are needed to confirm these hypotheses.

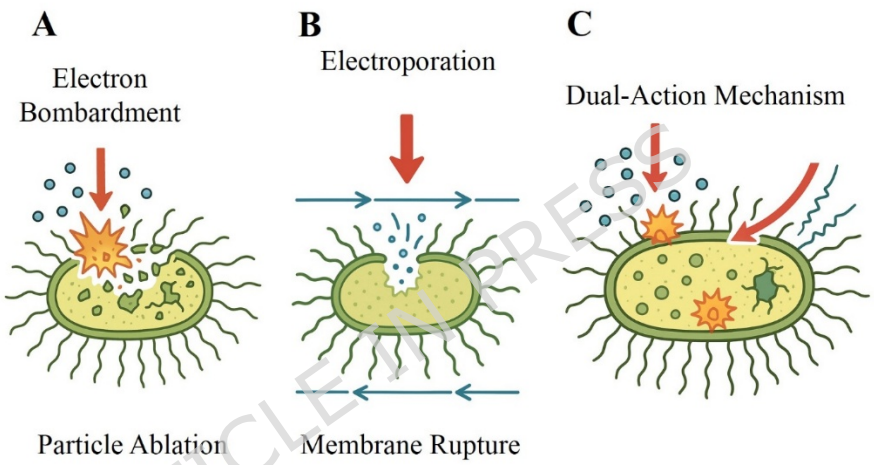


Figure 6: Proposed dual-action mechanism of airborne multidrug-resistant (MDR) bacterial inactivation via Electron-Beam Irradiation (EBI). (A) Direct physical electron bombardment leading to localized outer membrane ablation and structural fragmentation. (B) Electroporation-induced stress resulting in localized membrane rupture, structural collapse, and intracellular leakage. (C) The synergistic dual-action pathway combining mechanical disruption and electrostatic field-induced envelope compromise, leading to total cellular inactivation.

This study has certain limitations that should be acknowledged. The bacterial reduction levels observed may have been negatively influenced by

ARTICLE IN PRESS

the high humidity produced by the nebulizer during aerosolization. Elevated moisture can temporarily reduce electrostatic activity and charge-transfer interactions within the electron discharge field, which may have decreased the disinfection efficacy. This humidity effect reflects the experimental setup and is not necessarily representative of typical indoor environments, where lower relative humidity is more common [42, 43].

Additionally, bacterial aerosols were generated from suspensions in 0.9% (w/v) physiological saline. While this is a standard laboratory practice for maintaining cell viability, it may not fully represent the complex chemical composition of natural respiratory droplets or other clinical matrices (such as saliva or sink-derived aerosols) in which these pathogens are transmitted in healthcare settings. The composition of the suspending medium can influence aerosol droplet evaporation, particle size distribution, and bacterial inactivation kinetics.

ARTICLE IN PRESS

Furthermore, a 3-jet Collison nebulizer was used to generate the bacterial aerosols. Although widely employed in bioaerosol research, Collison nebulizers can impose mechanical shear stress that may damage bacterial cell membranes prior to EBI exposure. This pre-treatment effect could have contributed, at least partially, to the morphological changes observed in the SEM images and to the overall inactivation efficiency.

In addition, the maximum $\log_{10}$ reduction achieved may have been limited by the inoculum concentration tested. Future studies should investigate the

ARTICLE IN PRESS

performance of the EBI system using more clinically relevant suspending fluids (e.g., artificial saliva), gentler aerosol generation methods, and higher microbial challenge concentrations under stricter containment conditions.

5. Conclusions

In summary, the electron-beam irradiation (EBI) system represents a promising technology for mitigating airborne infections and indoor air decontamination. Its chemical-free operation enables continuous inactivation of airborne microorganisms and offers a practical strategy for reducing exposure to multidrug-resistant bacterial aerosols. Therefore, in healthcare, laboratory, and other high-risk environments, EBI-based air treatment has the potential to contribute meaningfully to the prevention of hospital-acquired infections, especially among vulnerable patient populations. Quantitative microbial reductions, combined with consistent qualitative trends of surface-level morphological disruption, indicate that the system initiates rapid, physical and electrical cellular stress. Future research should investigate the molecular and genetic consequences of EBI exposure. Studies on bacterial gene expression will clarify how electron-beam irradiation influences biofilm formation, antibiotic resistance behavior, susceptibility to other disinfection methods, and overall pathogenicity. In parallel, analyses of intracellular components, including DNA integrity and chromosomal organization, are needed to determine how electron beam-induced damage mechanisms affect genetic material and

ARTICLE IN PRESS

internal structures. These investigations will extend evaluation from outer envelope alterations to fundamental cellular and molecular pathways, providing deeper insight into the biological impact of EBI treatment. In addition, further evaluation under a wider range of environmental conditions, together with expanded testing against viral and fungal aerosols, will help define the broad antimicrobial spectrum of EBI and enhance its suitability for real-world infection-control applications.

Declarations

Ethics approval and consent to participate:

All experiments and methods were carried out in accordance with relevant guidelines and regulations. The experimental protocols were approved by the Ethics Committee of Iran University of Medical Sciences (Approval ID: IR.IUMS.REC.1403.958). Informed consent was obtained from all subjects and/or their legal guardian(s).

ARTICLE IN PRESS

Data availability

The data used and/or analyzed during the current study are available from the corresponding author upon reasonable request.

Acknowledgments

The authors would like to acknowledge the facilities, as well as the scientific and technical assistance, provided by the Antimicrobial Research Center

ARTICLE IN PRESS

under the Institute of Immunology and Infectious Diseases at Hazrat-e Rasoul Hospital, Iran University of Medical Sciences. We also appreciate Rahavard Fanavari Company for all helps and its technical support during the project. Authors also acknowledge Professor Kirstin Ross and Professor Harriet Whiley from Flinders University and their role in providing guidance on experimental design and constructive feedback during manuscript editing. Moreover, the authors used the ChatGPT language model (GPT-4, OpenAI, San Francisco, CA, USA) to assist with formal English writing and grammar correction during manuscript preparation. All content was reviewed and approved by the authors.

ARTICLE IN PRESS

Funding

This study was funded by the Antimicrobial Resistance Research Center of the Institute of Immunology and Infectious Diseases at Hazrat Rasoul Hospital, Iran University of Medical Sciences (Grant number REC.1403.958). Plasma Shield Ltd (Australia) provided additional support limited to publication-related costs and providing funding to researchers at Flinders University, Australia to provide an external and independent review of the study design.

Conflicts of Interest

Both funders had no role in the conduct of the experimental work including selection of test organisms, data collection or analysis, interpretation of the

ARTICLE IN PRESS

results, decision to publish, or preparation of the manuscript. The authors declare that they have no conflicts of interest.

References

[1] CDC Winnable Battles Final Report: Healthcare-associated infections (HAIs)., Centers Dis. Control Prev. (2017). https://stacks.cdc.gov/view/cdc/43072/cdc_43072_DS1.pdf?

[2] F.B. Solomon, F. Wadilo, E.G. Tufa, M. Mitiku, Extended spectrum and metalo beta-lactamase producing airborne Pseudomonas aeruginosa and Acinetobacter baumanii in restricted settings of a referral hospital: a neglected condition, Antimicrob. Resist. Infect. Control. 6 (2017) 106.

[3] A.M. Jones, J.R.W. Govan, C.J. Doherty, M.E. Dodd, B.J. Isalska, T.N. Stanbridge, A.K. Webb, Identification of airborne dissemination of epidemic multiresistant strains of Pseudomonas aeruginosa at a CF centre during a cross infection outbreak, Thorax. 58 (2003) 525–527.

[4] P. Mc Gann, T.L. Luo, M.J. Martin, H.D. Dao, V. Kovalchuk, V. Kondratiuk, I. Kovalenko, B.J. Plaza, J.M. Kettlewell, C.P. Anderson, J.R. Smedberg, A.C. Ong, R. Maybank, Y.I. Kwak, J.S. Hawley-Molloy, F. Lebreton, J.W. Bennett, Foreign Combatants Wounded in Ukraine Colonized by Extensively Drug-Resistant Organisms: A Potential Source of Global Dissemination, J. Infect. Dis. (2025) jiaf538. doi:10.1093/infdis/jiaf538.

[5] R.F. Chemaly, S. Simmons, C. Dale Jr, S.S. Ghantoji, M. Rodriguez, J. Gubb, J. Stachowiak, M. Stibich, The role of the healthcare environment in the spread of multidrug-resistant organisms: update on current best practices for containment, Ther. Adv. Infect. Dis. 2 (2014) 79–90.

[6] B. Wen, F. Lei, Transmission routes and prevention strategies of multidrug-resistant organism infections in hospitals, J. Mod. Med. Nurs. 1 (2024).

[7] P.Y. Chia, S. Sengupta, A. Kukreja, S. SL Ponnampalavanar, O.T. Ng, K. Marimuthu, The

ARTICLE IN PRESS

role of hospital environment in transmissions of multidrug-resistant gram-negative organisms, Antimicrob. Resist. Infect. Control. 9 (2020) 29.

[8] S.C. Wong, J.H. Chen, M.O. Kwok, C.Y. Siu, L.L. Yuen, C.H. AuYeung, C.K. Li, B.H. Li, B.W. Chan, S.Y. So, Air dispersal of multi-drug-resistant organisms including meticillin-resistant Staphylococcus aureus, carbapenem-resistant Acinetobacter baumannii and carbapenemase-producing Enterobacterales in general wards: surveillance culture of air grilles, J. Hosp. Infect. 149 (2024) 26–35.

[9] N.J. Bolister, H.E. Johnson, C.M. Wathes, The ability of airborne Klebsiella pneumoniae to colonize mouse lungs, Epidemiol. Infect. 109 (1992) 121.

[10] N.M. Barnes, H. Wu, Mechanisms regulating the airborne survival of Klebsiella pneumoniae under different relative humidity and temperature levels, Indoor Air. 32 (2022) e12991.

[11] S.H. Mirhoseini, M. Nikaeen, Z. Shamsizadeh, H. Khanahmad, Hospital air: A potential route for transmission of infections caused by β-lactam–resistant bacteria, Am. J. Infect. Control. 44 (2016) 898–904.

[12] D. Bommu, Comparative Study on High-Efficiency Particulate Air (Hepa) Filters for Enhancing Hospital Indoor Air Quality, (2020).

[13] S. Sorouri, H. Ahmari Tehran, M. Parhoon, M. Saeidi, Air pollution in hospitals: a critical public health emergency and strategies for improving indoor air quality and patient safety, Heal. Provid. 5 (2025) 15–34.

[14] D.P. Regan, C. Fong, A.C.S. Bond, C. Desjardins, J. Hardcastle, S.-H. Hung, A.P. Holmes, J.D. Schiffman, M.S. Maginnis, C. Howell, Improved recovery of captured airborne bacteria and viruses with liquid-coated air filters, ACS Appl. Mater. Interfaces. 14 (2022) 50543–50556.

[15] H. Mittal, S.R. Parks, T. Pottage, J.T. Walker, A.M. Bennett, Survival of microorganisms on HEPA filters, Appl. Biosaf. 16 (2011) 163–166.

ARTICLE IN PRESS

ARTICLE IN PRESS

[16] R.A. Santos, A.M. Hasslocher-Moreno, study of the microbiological efficiency of a hospital ventilation system with hepa filtration in the prevention of airborne pathogens, Rev. Gestão Soc. e Ambient. 18 (2024) 1–20.

[17] S.D. Lowther, W. Deng, Z. Fang, D. Booker, J.D. Whyatt, O. Wild, X. Wang, K.C. Jones, Factors affecting real-world applications of HEPA purifiers in improving indoor air quality, Environ. Sci. Adv. 2 (2023) 235–246.

[18] M.H. Ereth, D.H. Hess, A. Driscoll, M. Hernandez, F. Stamatatos, Particle control reduces fine and ultrafine particles greater than HEPA filtration in live operating rooms and kills biologic warfare surrogate, Am. J. Infect. Control. 48 (2020) 777–780.

[19] D.T. Liu, K.M. Phillips, M.M. Speth, G. Besser, C.A. Mueller, A.R. Sedaghat, Portable HEPA purifiers to eliminate airborne SARS-CoV-2: a systematic review, Otolaryngol. Neck Surg. 166 (2022) 615–622.

[20] F. Liu, Q. Ma, M.M. Marjub, A.K. Suthammanont, S. Sun, H. Yao, Y. Tao, W. Zhang, Reactive air disinfection technologies: principles and applications in bioaerosol removal, ACS ES&T Eng. 3 (2023) 602–615.

[21] A. Kumar, P. Verma, R. Kaushik, Photocatalytic inactivation and disinfection of bioaerosols: a review, Environ. Chem. Lett. (2025) 1–23.

[22] C.F. Green, P. V Scarpino, The use of ultraviolet germicidal irradiation (UVGI) in disinfection of airborne bacteria, Environ. Eng. Policy. 3 (2001) 101–107.

[23] G. Mainelis, Collection of airborne microorganisms by electrostatic precipitation, Aerosol Sci. Technol. 30 (1999) 127–144.

[24] A. Vohra, D.Y. Goswami, D.A. Deshpande, S.S. Block, Enhanced photocatalytic disinfection of indoor air, Appl. Catal. B Environ. 64 (2006) 57–65.

[25] R. Jangra, K. Ahlawat, M.K. Mohan, R. Prakash, Indoor air disinfection by non thermal atmospheric pressure plasma: a comparative study of performance in low and high humidity environments, Phys. Scr. 99 (2024) 85612.

ARTICLE IN PRESS

ARTICLE IN PRESS

[26] Y. Xu, A. Bassi, Non-thermal plasma decontamination of microbes: a state of the art, Biotechnol. Prog. 41 (2025) e3511.

[27] S. Tao, Y. Zhu, M. Chen, W. Shangguan, Advances in electrostatic plasma methods for purification of airborne pathogenic microbial aerosols: Mechanism, modeling and application, Environ. Heal. 2 (2024) 596–617.

[28] H. Whiley, T.P. Keerthirathne, E.J. Kuhn, M.A. Nisar, A. Sibley, P. Speck, K.E. Ross, Efficacy of the PlasmaShield®, a non-thermal, plasma-based air purification device, in removing airborne microorganisms, Electrochem. 3 (2022) 276–284.

[29] T. Roth, E. Zelinger, T. Kossovsky, G. Borkow, Scanning electron microscopy analysis of biofilm-encased bacteria exposed to cuprous oxide-impregnated wound dressings, Microbiol. Res. (Pavia). 15 (2024) 2358–2368.

[30] A.R. Sofy, A.A. Hmed, A.M.A. Sharaf, K.A. El-Dougdoug, Structural changes of pathogenic multiple drug resistance bacteria treated with T. vulgaris aqueous extract, Nat. Sci. 12 (2014) 83–88.

[31] Y. Sun, Z. Zhang, S. Wang, Study on the bactericidal mechanism of atmospheric-pressure low-temperature plasma against Escherichia coli and its application in fresh-cut cucumbers, Molecules. 23 (2018) 975.

[32] F. Pillet, C. Formosa-Dague, H. Baaziz, E. Dague, M.-P. Rols, Cell wall as a target for bacteria inactivation by pulsed electric fields, Sci. Rep. 6 (2016) 19778.

[33] G. Duan, Y. Zhang, B. Luan, J.K. Weber, R.W. Zhou, Z. Yang, L. Zhao, J. Xu, J. Luo, R. Zhou, Graphene-induced pore formation on cell membranes, Sci. Rep. 7 (2017) 42767.

[34] M. Dezest, A.-L. Bulteau, D. Quinton, L. Chavatte, M. Le Bechec, J.P. Cambus, S. Arbault, A. Nègre-Salvayre, F. Clement, S. Cousty, Oxidative modification and electrochemical inactivation of Escherichia coli upon cold atmospheric pressure plasma exposure, PLoS One. 12 (2017) e0173618.

ARTICLE IN PRESS

ARTICLE IN PRESS

[35] C. Du, Y. Liu, Y. Huang, Z. Li, R. Men, Y. Men, J. Tang, Qualitation and quantitation on microplasma jet for bacteria inactivation, Sci. Rep. 6 (2016) 18838.

[36] Z.-Y. Huo, Y.-J. Kim, I.-Y. Suh, D.-M. Lee, J.H. Lee, Y. Du, S. Wang, H.-J. Yoon, S.-W. Kim, Triboelectrification induced self-powered microbial disinfection using nanowire-enhanced localized electric field, Nat. Commun. 12 (2021) 3693.

[37] P. Estifaee, X. Su, S.K. Yannam, S. Rogers, S.M. Thagard, Mechanism of E. coli inactivation by direct-in-liquid electrical discharge plasma in low conductivity solutions, Sci. Rep. 9 (2019) 2326.

[38] T. Barkhade, K. Nigam, G. Ravi, S. Rawat, S.K. Nema, Investigating the effects of microwave plasma on bacterial cell structures, viability, and membrane integrity, Sci. Rep. 15 (2025) 18052.

[39] J. Zhao, J. Qian, H. Zhuang, J. Luo, M. Huang, W. Yan, J. Zhang, Effect of plasma-activated solution treatment on cell biology of Staphylococcus aureus and quality of fresh lettuces, Foods. 10 (2021) 2976.

[40] S.-K. Yeo, M.-T. Liong, Effects and applications of sub-lethal ultrasound, electroporation and UV radiations in bioprocessing, Ann. Microbiol. 63 (2013) 813–824.

[41] Y. Ma, W. Zhu, G. Zhu, Y. Xu, S. Li, R. Chen, L. Chen, J. Wang, Efficient robust yield method for preparing bacterial ghosts by Escherichia coli phage ID52 lysis protein E, Bioengineering. 9 (2022) 300.

[42] J.T. Park, T. Uehara, How bacteria consume their own exoskeletons (turnover and recycling of cell wall peptidoglycan), Microbiol. Mol. Biol. Rev. 72 (2008) 211–227.

[43] P.R. Sreedevi, K. Suresh, Cold atmospheric plasma mediated cell membrane permeation and gene delivery-empirical interventions and pertinence, Adv. Colloid Interface Sci. 320 (2023) 102989.

[44] Z.-Y. Huo, G.-Q. Li, T. Yu, C. Feng, Y. Lu, Y.-H. Wu, C. Yu, X. Xie, H.-Y. Hu, Cell

ARTICLE IN PRESS

ARTICLE IN PRESS

transport prompts the performance of low-voltage electroporation for cell inactivation, Sci. Rep. 8 (2018) 15832.

[45] L. Han, S. Patil, D. Boehm, V. Milosavljević, P.J. Cullen, P. Bourke, Mechanisms of inactivation by high-voltage atmospheric cold plasma differ for Escherichia coli and Staphylococcus aureus, Appl. Environ. Microbiol. 82 (2016) 450–458.

[46] L. Patinglag, L.M. Melling, K.A. Whitehead, D. Sawtell, A. Iles, K.J. Shaw, Non-thermal plasma-based inactivation of bacteria in water using a microfluidic reactor, Water Res. 201 (2021) 117321.

ARTICLE IN PRESS